EASR

Engineering and Applied Science Research

https://www.tci-thaijo.org/index.php/easr/index

Published by the Faculty of Engineering, Khon Kaen University, Thailand

Landslide susceptibility assessment using frequency ratio model at Ossey watershed area in Bhutan

Thongley Thongley and Chaiwiwat Vansarochana*

Faculty of Agriculture, Natural Resources and Environment, Naresuan University, Phitsanulok 65000, Thailand

Received 20 April 2020
Revised 16 June 2020
Accepted 23 June 2020

Abstract

Landslide is one of the most frequent disaster at Ossey watershed area in Bhutan causing inconvenience to the local people, financial losses and claiming lives of the people every year. This study aimed at developing the landslide susceptibility map (LSM) based on its severity at Ossey watershed area in Bhutan. During the landslide inventory, a total of 164 landslide locations were identified using the sentinel-2 interpretation, google earth image and field survey which was divided into training and validation dataset. Training and validation dataset comprise of 70% (115 locations) and 30% (49 locations) of the total landslide, respectively. Twelve factors were considered for this study which includes altitude, aspect, curvature, slope gradient, topographic wetness index, stream power index, normalized difference vegetation index, proximity to road, proximity to river, lithology, rainfall data, and land cover map. The landslide susceptibility map was developed using the frequency ratio model. The kappa index was used for the checking reliability of the model and area under curve (AUC) of the receiver operating characteristics (ROC) curve was used for validation of the LSM. The kappa indexes were 0.4261 and 0.5510 for training and validation dataset respectively indicating the LSM is reliable as the kappa values fall under the scale of moderately reliable. The AUC are 0.7916 and 0.8742 for the success rate and prediction rate respectively indicating the LSM is accurate enough for the engineering application. The final LSM is classified into five classes using equal interval classifier as the data distributions are close to the normal. The final LSM could be useful for the future researchers, planners, decision makers and engineers for the future developmental activities.

Keywords: Landslide susceptibility mapping, Frequency ratio model, Area under curve, Kappa index

1. Introduction

Landslide is defined as the movement of the slope forming materials composed of natural, artificial and combination of these material from its original position [1]. Landslides is one of the most frequent and destructive disaster in the mountainous area [2]. Landslide cause damage to various engineering structure, agricultural land, mining sites, forest, residential areas and even claim lives of thousands of people [3]. According to the data released by the international disaster database EM-DAT (https://www.emdat.be/emdat_db/), 7969887 people were affected, and 21022 people were killed by landslides in Asia alone from 1900-2019. It is important to develop systematic methodology to prevent and control the landslide disaster in the future. Generally, a landslides susceptibility map is the first step to inform the decision makers for the future infrastructure development [4].

There are several qualitative and quantitative approaches to study the relationship between the landslide and the factors [5]. The qualitative approaches are entirely based on the judgment of the person carrying out the research or based on expert's evaluation. The input data are usually derived from field visit assessment and aerial photo interpretation [6]. The quantitative approaches are based on the numerical calculation between landslide events and the factors [5]. The quantitative approaches are classified into statistical approaches, geotechnical engineering approaches and neural network analysis[6]. In the last few decades, statistical approaches was popular among the various approaches [2]. Statistical are classified into bivariate and multivariate. In bivariate statistical approach, the factors are compared with landslide event map and derive the weight of the classes of the all the factors on the basis of landslide density [6]. The bivariate statistical approaches include Frequency ratio [7], index of entropy [8], information value [9], statistical index [10], certainty factor [11] and weight of evidence [12]. Although there are many approaches for the multivariate statistics, the most popular approach is logistic regression [2].

Bhutan is characterized by steep and rugged terrain which is heavily affected by the landslides during monsoon season. Although the country is one of the most landslide prone area, there isn't much study done on landslides in Bhutan. Few researches on landslides in Bhutan covers only certain portion of Bhutan, that doesn't cover the most landslide prone area. The few studies carried out on landslide in Bhutan includes landslide susceptibility mapping using information value at Phuntsholing by Pasang and Kubíček [13], determination of probabilities of landslide event-a case study of Bhutan by Sarkar and Dorji [14], application of soil nailing for the landslide mitigation in Bhutan: A case study at Sorchen Bypass by Sarkar et al. [15] and method for landslide risk evaluation and road operation management: A case study of Bhutan by Cheki and Shibayama [16]. Although

*Corresponding author.
Email address: Chaiwiwatv@gmail.com
doi: 10.14456/easr.2021.7

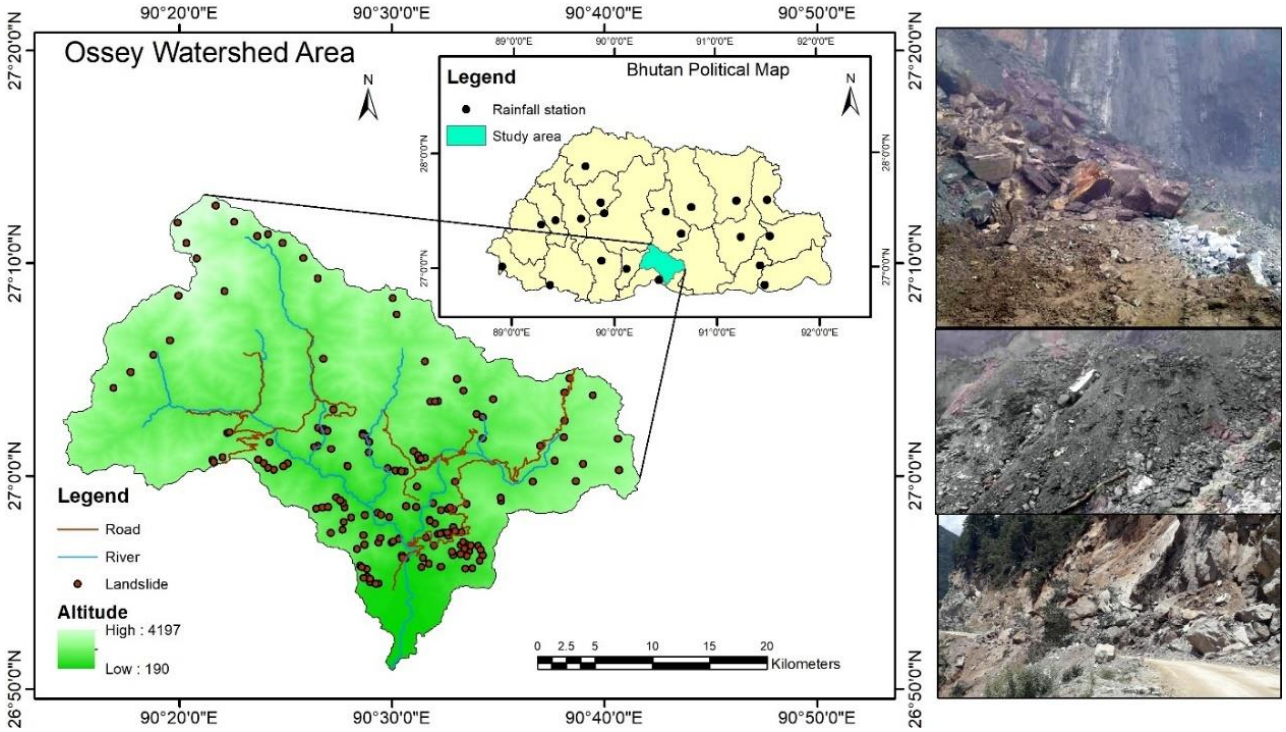

Figure 1 The location of rainfall stations and landslide locations at Ossey watershed area

Ossey watershed area is one of the most landslide prone area in Bhutan, there is no study on landslides covering this area.

The purpose of this study was to find the accurate landslide potential area in the future at Ossey watershed area and to zone the landslides area based on its severity. The study also aimed to derive weight of the individual classes of the factor using the frequency ratio model. The developed LSM could serve as an effective guide for the future developmental activities.

2. Materials and methods

2.1 Study area

The Ossey watershed (Figure 1) is located in the southern part of Bhutan with an area of approximately 820sq.km. It is located in between 26°50'00"N-27°15'00"N latitude and 90°10'00"E-90°50'00"E longitude and at an altitude of 190m-4194m above the mean sea level. The average annual precipitation is 3950mm and the maximum slope gradient is 72°. The average temperature ranges from 19°C in winter to 27°C in summer. The weak lithological factor and favorable hydrological environment of the terrain causes slope failure every year. The area experiences number of landslides during the monsoon season due to intense precipitation.

2.2 Landslide inventory mapping

The identification and training the existing landslide is fundamental step to find the relationship between landslide distribution and its factors [17]. The accuracy of landslide assessment depend on the amount, distribution and training existing landslides [10]. In this study, the landslide inventory was done using sentinel-2 interpretation, google earth image and the extensive field survey using handheld GPS during the monsoon season of the year 2017 to 2019. A total of 164 landslides were identified during the landslides inventory (Figure 1). As per the suggestion of the Liu and Duan [10] and Shirani et al. [3], the landslide inventory were divided into 70%(115 locations) and 30% (49 locations) for training and validation dataset respectively.

2.3 Landslide factor preparation

It is essential to use appropriate landslide factors for the landslide assessment [18]. A total of twelve factors were employed for this study. These factors were altitude, slope gradient, slope aspect, slope curvature, topographic wetness index (TWI), stream power index (SPI), normalized difference vegetation index (NDVI), land cover, proximity to river, proximity to road, Lithology and rainfall. The SRTM (30m) was used for the extraction of aspect, curvature, elevation, slope angle, SPI and TWI. The Geological map of Bhutan(1:500000) prepared by Long, McQuarrie, Tobgay, Grujic, and Hollister [19] was used for the extraction of lithological map. The sentinel(10m) was used for the preparation of land cover map and NDVI. The digital topographic map (1:25000) prepared by Japan Internation Cooperation Agency (JICA) was used for extraction of proximity to river and road. All the factors were resampled to grid of 30mx30m which is same as the spatial resolution of SRTM DEM and stored in the grid format. The study area consist of 1376 row by 1497 columns with total of 911947 grid cell (820,752,300m^2). The detail of individual landslide factors were elaborated in the following section.

Regarding the altitude, it doesn't influence on the landslide event directly. However, it affects the intensity of rainfall, humidity and tectonic setting of an area [18]. The varying lithology with the change in altitude also impact the landslides probability [20]. These causes differences in the landslide event. The classified altitude map is shown in the Figure 2(a).

In the case of slope gradient, as the slope gradient increased, the shear stress of the soil also increased indicating higher landslide probability in the steeper slope [21]. The slope gradient is classified into five classes as shown in the Figure 2(b).

The horizontal direction of the slope face is called slope aspect [22]. The different directions of the slopes receives different amount of rainfall and solar radiation [17]. The probability of the landslides vary from one face of the slope to other [21]. The slope aspect map is classified as shown in the Figure 2(c).

The slope curvature is the rate of change of terrains or aspect [17]. The terrain is said to be convex when its curvature value is positive and concave terrain when its value is negative. The

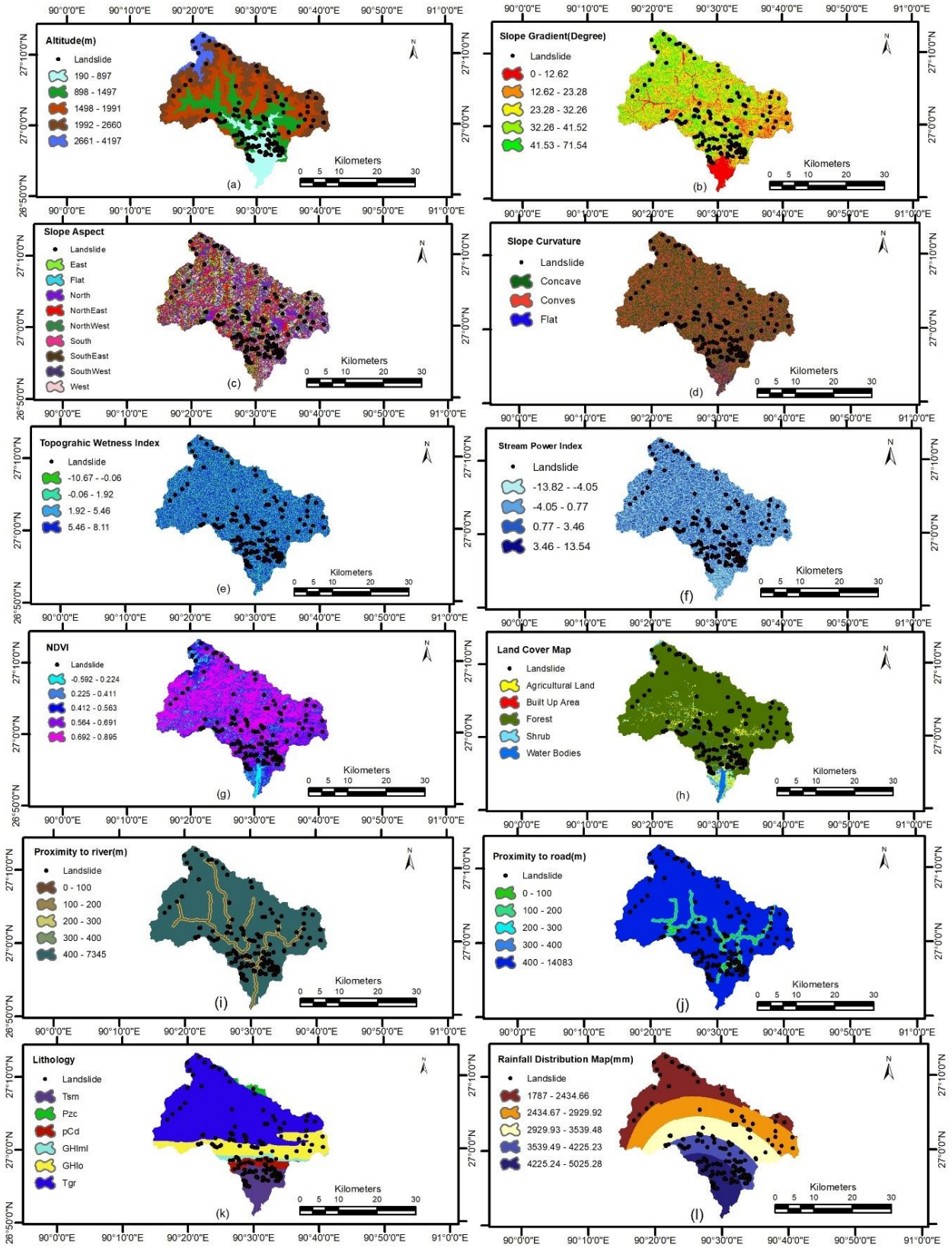

Figure 2 Factors (a) Altitude (b) Slope Gradient (c) Slope Aspect (d) Slope Curvature (e) Topographic wetness Index (f) Stream Power Index (g) Normalized Difference Vegetation Index (h) Land cover Map (i) Proximity to river (j) Proximity to road (k) Lithology (l) Rainfall distribution map

curvature is said to be flat, when its value is in between -0.05 to 0.05 [18]. The slope curvature is as shown in the Figure 2(d).

The topographic wetness index (TWI) indicate the amount of water accumulation at any point in an area [2]. The classified TWI is shown in the Figure 2(e) and it is calculated using the equation given by Moore, Grayson, and Ladson [23].

$$TWI = ln\left(\frac{\alpha}{tan\beta}\right) \quad (1)$$

Where α is the upslope contributing area and β is the slope angle.

Stream power index (SPI) measures the erosive capacity of the flowing water in the study area [2]. It assumes that the water discharge is proportional to the specific catchment area [17]. The SPI is calculated based on equation given by Moore et al. [23]

$$SPI = A_s tan\,\beta \quad (2)$$

Where, *As* is the specific catchment area and β is the slope gradient in degrees.

The vegetation root stabilizes the terrain and reduces landslides. When the NDVI value is high, the vegetation is proved to be healthy [18]. For this study, the red and near-infrared bands of the sentinel-2 is used for the calculation of NDVI. The NDVI value ranges from -1 to 1. The Figure 2(g) shows the NDVI classes.

The occurrence of the landslide differs for different types of land cover. The anthropogenic activities alters the slope stability and triggers the landslides [4]. Generally, the landslide are more prominent in an area characterized by inclined and mountainous area [21]. The different types of land use and land cover are shown in the Figure 2(h).

The tides of the river erodes its bank which eventually destabilize the toe of the slope. Normally, the area closer to the river experiences more landslides than the area far from the river [2]. The Figure 2(i) shows the classes of proximity to river.

The road construction cut the toe of the slope which induces slope instability [5]. The destabilized slope has higher chances of landslide occurrence. The classified proximity to road is as shown in the Figure 2(j).

Different composition and structure of lithology has different strength, permeability and erosional effect [3]. The low strength lithology has higher chance of detachment from the slope. Lithology plays an important role in a landslide's size, frequency and type [4]. The detail of lithological units are elaborated in the Table 1 and shown in Figure 2(k).

Table 1 Description of lithological unit

Geologic age	Code	Lithology
Miocene-Pliocene	Tsm	Sandstone and cobble-conglomeratic sandstone
Paleoproterozoic	pCd	Schist, phyllite, quartzite and limestone.
Ordovician or younger	Pzc	Micaceous quartzite, schist, marble, phyllite, and phyllitic quartzite.
Neoproterozoic-Cambrian	GHlml	quartzite, schist, kyanite, sillimanite and staurolite
Cambrian-Ordovician	GHlo	Granite, schist, and quartzite and granite
Miocene	Tgr	Massive to foliated, syn-Himalayan leucogranite plutons.

Table 2 Weight of the classes of the factors using frequency ratio

Factor	Class	No of Pixel in domain	% of Domain	Number of Landslide	% of Landslide	Frequency Ratio
Altitude (m)	190 - 897	123321	13.52	45	39.13	2.89
	897 - 1497	222051	24.35	31	26.96	1.11
	1497 - 1991	294483	32.29	21	18.26	0.57
	1991 - 2660	223435	24.50	13	11.30	0.46
	2660 - 4197	48657	5.34	5	4.35	0.81
Slope gradient (Degree)	0 - 12.62	88489	9.70	6	5.22	0.54
	12.62 - 23.28	208452	22.86	20	17.39	0.76
	23.28 - 32.26	275837	30.25	28	24.35	0.80
	32.26 - 41.52	239515	26.26	29	25.22	0.96
	41.52 - 71.53	99654	10.93	32	27.83	2.55
Slope Aspect	Flat	285	0.03	0	0.00	0.00
	North	118174	12.96	6	5.22	0.40
	NorthEast	97997	10.75	9	7.83	0.73
	East	110602	12.13	14	12.17	1.00
	SouthEast	129200	14.17	33	28.70	2.03
	South	120454	13.21	18	15.65	1.19
	SouthWest	126820	13.91	18	15.65	1.13
	West	111498	12.23	7	6.09	0.50
	NorthWest	96917	10.63	10	8.70	0.82
Slope Curvature	Concave	434525	47.65	70	60.87	1.28
	Flat	36424	3.99	3	2.61	0.65
	Convex	440998	48.36	42	36.52	0.76
TWI	-10.67 - -0.06	80173	8.79	10	8.70	0.99
	-0.06 - 1.92	245561	26.93	35	30.43	1.13
	1.92 - 5.46	126394	13.86	18	15.65	1.13
	5.46 - 8.11	459819	50.42	52	45.22	0.90
SPI	-13.81 - -4.05	233485	25.60	18	15.65	0.61
	-4.05 - 0.77	323339	35.46	41	35.65	1.01
	0.77 - 3.45	292178	32.04	41	35.65	1.11
	3.45 - 13.54	62945	6.90	15	13.04	1.89
NDVI	-0.592 - 0.224	39044	4.28	22	19.13	4.47
	0.224 - 0.411	101937	11.18	28	24.35	2.18
	0.411 - 0.562	150158	16.47	17	14.78	0.90
	0.562 - 0.690	267052	29.28	27	23.48	0.80
	0.690 - 0.895	353756	38.79	21	18.26	0.47

Table 3 (continued) Weight of the classes of the factors using frequency ratio

Factor	Class	No of Pixel in domain	% of Domain	Number of Landslide	% of Landslide	Frequency Ratio
Land Cover	Agricultural Land	29903	3.28	2	1.74	0.53
	Built Up Area	851	0.09	0	0	0
	Forest	844305	92.58	110	95.65	1.03
	Shrub	22629	2.48	3	2.61	1.05
	Water Bodies	14259	1.56	0	0	0
Proximity to River	0-100	31639	3.47	7	6.09	1.75
	100-200	27341	3.00	1	0.87	0.29
	200-300	29785	3.27	4	3.48	1.06
	300-400	25379	2.78	4	3.48	1.25
	400<	797803	87.48	99	86.09	0.98
Proximity to Road	0-100	30136	3.30	5	4.35	1.32
	100-200	22593	2.48	3	2.61	1.05
	200-300	23374	2.56	6	5.22	2.04
	300-400	19606	2.15	1	0.87	0.40
	400<	816238	89.50	100	86.96	0.97
Lithology	Tsm	96424	10.57	32	26.02	2.46
	Pzc	9617	1.05	1	0.87	0.82
	pCd	34574	3.79	12	10.43	2.75
	GHlml	22953	2.52	5	4.35	1.73
	GHlo	162532	17.82	23	20.00	1.12
	Tgr	585847	64.24	42	36.52	0.57
Rainfall	1787.00 - 2434.65	233537	25.61	19	16.52	0.65
	2434.65 - 2929.92	260302	28.54	14	12.17	0.43
	2929.92 - 3539.48	185098	20.30	17	14.78	0.73
	3539.48 - 4225.23	123336	13.52	39	33.91	2.51
	4225.23 - 5025.27	109674	12.03	26	22.61	1.88

The rainfall is one of the important triggering factor for the landslides. The rainfall infiltrates in the terrain and triggers the erosion [2]. Generally, the area with higher rainfall experiences more landslides. For this study, the average annual rainfall map was developed using 21 years (1996-2017) data from 20 rainfall stations (Figure 1) of Bhutan and the inverse distance weighting (IDW) technique was applied for the interpolation. Since the rainfall data are collected at the rain gauge stations, it will be in the form of point feature. The interpolation technique is necessary for generating the rainfall map of the study area. The IDW interpolation estimates the unknown rainfall from the known data from the stations that are adjacent to the unknown area [24]. The IDW interpolation assumes that the value of the unsampled point is the linear weighted average of the known values within the neighborhood [24]. The influence on the output value becomes minimal as the distance increases from the known point [25]. The IDW interpolated rainfall map will help in finding the spatial relationship between the landslides and the rainfall. The Figure 2(l) shows the classified average annual rainfall distribution using IDW interpolation.

2.4 Frequency ratio model

Frequency Ratio (FR) model creates relationship between existing landslides with the individual classes of the factors [18]. FR assumes that the landslides are determined by its factors and the future landslides occurs under the same condition as that of past landslides [26]. The FR is defined as the ratio of percentage of the landslides in the individual class to the percentage of pixel in the class of the factor and its calculated using the Equation 3 [22]. If the influence of the class of a factor is strong, the FR value will be greater than one and vice versa [26]. The Table 2 shows the FR values for the individual classes of the factors.

$$FR = \frac{\frac{N_p(LX_i)}{\sum_{i=1}^{m} N_p(LX_i)}}{\frac{N_p(X_j)}{\sum_{j=1}^{m} N_p(X_j)}} \quad (3)$$

where, FR is the frequency ratio of class i of factor j, $Np(LX_i)$ is the number of pixels with landslides within class i of factor variable X, $Np(X_j)$ is the total number of pixel in the class of the factor X_j and m is the number of classes in the factor variable X_i. The Landslide Susceptibility Map (LSM) is calculated by summing up all the FR of all the factors.

$$LSM_{FR} = \sum FR \quad (4)$$

3. Results and discussion

3.1 Evaluation of influencing factor using frequency ratio value

The FR value shows the weight of the individual factor classes. The higher FR value indicates stronger correlation between the factor's class and landslides [18]. The Table 2 shows the FR value of the individual classes of the twelve factors calculated using the Equation 3.

As per the Table 2, the FR value decreases with increase in altitude. The altitude between 190m–897m and 897m – 1497m has a frequency ratio >1 while altitude above 1497m has FR<1. The similar pattern was observed by Jaafari, Najafi, Pourghasemi, Rezaeian, and Sattarian [27]. This result indicate that the probability of landslide occurrence is high in low altitude. This may be due to lithological units of the higher altitude are resistant to landslides [20]. Conversely, the frequency ratio value increases with the increase in the slope gradient. These shows that the landslide probability increases with slopes gradient [28]. The increase in slope gradient increases the shear stress of the soil and other associated unconsolidated materials.

For the slope aspect, the south facing slope has more frequency ratio value (FR>1) indicating more prone to landslides which includes southeast, southwest and east. The similar result was observed by Park et al. [28] and Meten, PrakashBhandary, and Yatabe [29]. Since the Ossey watershed area is located on the Himalayan region, the orographic effect of the giant Himalayan mountain brings more rainfall on the south facing slopes causing more landslides.

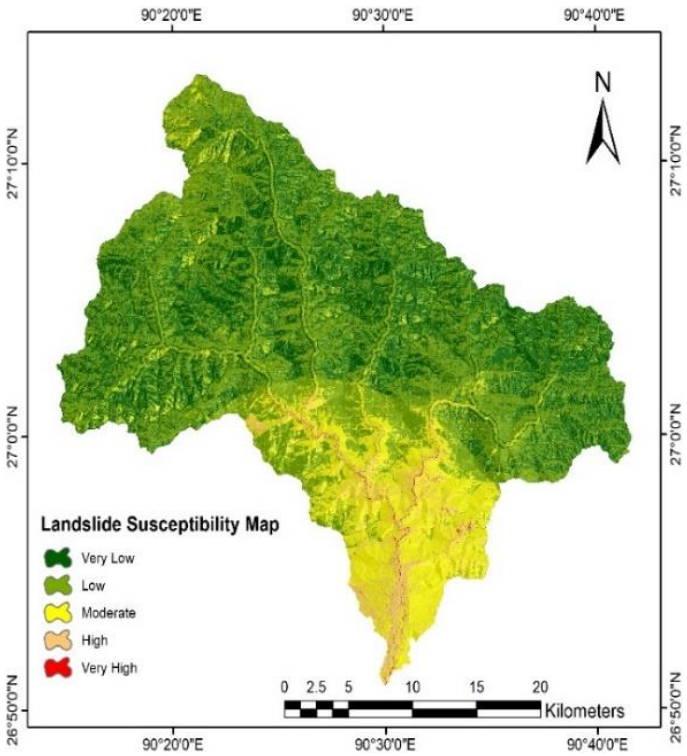

Figure 3 Landslide susceptibility map at Ossey watershed area

Regarding the slope curvature, the frequency ratio value of the concave slope is more than 1 indicating higher chances of the landslide, followed by convex and flat area. The previous study by Jaafari et al. [27] also shows similar results. These concave curvature terrains retain more moisture and reduces the stability causing more landslides. In the case of TWI, the landslide is more prominent in the TWI range -0.06 to 5.46 with FR value 1.13 (FR>1) while the TWI range -10 - -0.06 and 5.46 - 8.11 experiences less landslides with the FR value of 0.99.

The highest FR (1.89) corresponds to the highest SPI class 3.45-13.54. while lowest FR value (0.61) correspdonds to the lowest SPI class -13.81 - -0.405. İt is noticed that the FR value increases with increase in SPI value. Oppositely, the FR value decreases with increase in NDVI value. The lowest NDVI class (-0.592 - -0.224) has the highest FR value 4.47 indicating higher probability of landslides which coincides with barren area [22].

In the case of land use and land cover, the landslide are more prone in the shrubs and forest area with FR value of 1.05 and 1.03 respectively (FR>1) while there is no landslide in the built up area and water bodies which is true in the reality.

As for the proximity to river, the higher FR value (FR>1) coincide for the range 0 to 100m, 200m to 400m indicating more susceptible to landslides while the area beyond 400m has less FR value (FR<1) indicating safer place from the landslides. As the distance increase from the river, the probability of landslides is also minimal. Likewise, the higher FR value decreases with the increase in distance from the road. The highest FR value (FR>1) is observed upto the buffer distance of 300m from road. The FR value beyond 300m buffer from road is lesser than 1 indicating less chances of landslides. This may be due to instabilibity caused by the excavation during the road construction [7].

The lithological unit Tsm, pCd, GHlml and GHlo shows higher chance of landslide with FR weight 2.46, 2.75, 1.73 and 1.12 (FR>1) respectively. The unit Pzc and Tgr shows less likelihood for the landslide event with FR value 0.82 and 0.57 respectively.

The class having rainfall amount 3539.48mm to 5025.27mm has the higher FR (FR>1) while the classes from 1787mm to 3539.48mm has the lesser FR (FR<1). Clearly, it indicates that the landslides are proportional to the rainfall amount and agreeing to the fact that the landslides are also trigger by the rainfall [27].

3.2 Landslide susceptibility mapping

The factors were reclassified using the FR value from the Table 2. The LSM was developed by summing the reclassified factors using the Equation 4. The classification of LSM is necessary for the visual interpretation [27]. There are number of classification package in GIS software. The appropriate classification method is chosen based on the distribution of the landslide susceptibility value [5]. It is advisable to choose equal interval classifier, if the data distribution value is close to normal [27]. The equal interval classifier divides the range of attribute values into equal size sub-range [30]. For this LSM, the equal interval classifier was able to produce better visualization than the other classification. Therefore, considering the data value distribution and visualization, equal interval classification was used for this study as shown in the Figure 3.

The percentage of area covered by the different landslide susceptibility zones are shown in the Figure 4. As per the equal interval classification in the LSM, 32.18% (264.09km^2) of the total area falls in the very low susceptibility zone, 47.35% (388.61km^2) was located the low susceptibility area, 16.46% (135.08km^2) falls in the moderate susceptible area. The proportion of high and very high susceptibility zone are 3.82% (31.33km^2) and 0.20% (1.64km^2) of the total area respectively.

3.3 Evaluation of accuracy of landslide susceptibility mapping

It is important to evaluate the efficiency of the model and accuracy of the LSM [31]. The commonly used method for the validation is comparing the observed data (landslide inventory data) with the predicted data [3]. For this study, the landslides inventory data is divided into 70% (115 landslide points) for the training dataset and remaining 30% (49 landslide points) for the validation dataset. The equal number of non-landslide point is also identified for both training and validation dataset. Assign the value 1 for landslide point and 0 for non-landslide point for both training and validation dataset. The training dataset is used to

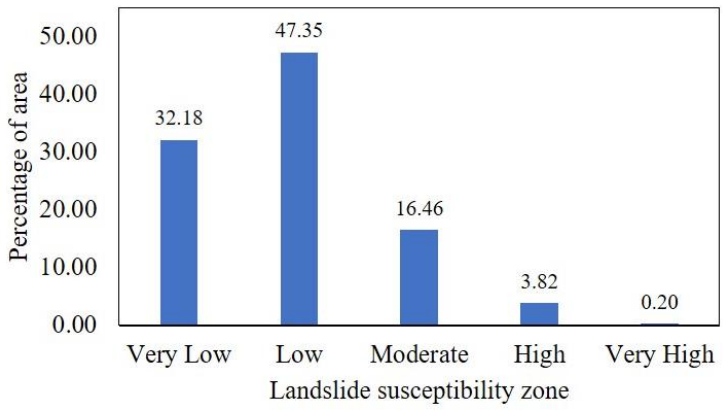

Figure 4 Percentage of area of the different zones of the landslide susceptibility mapping

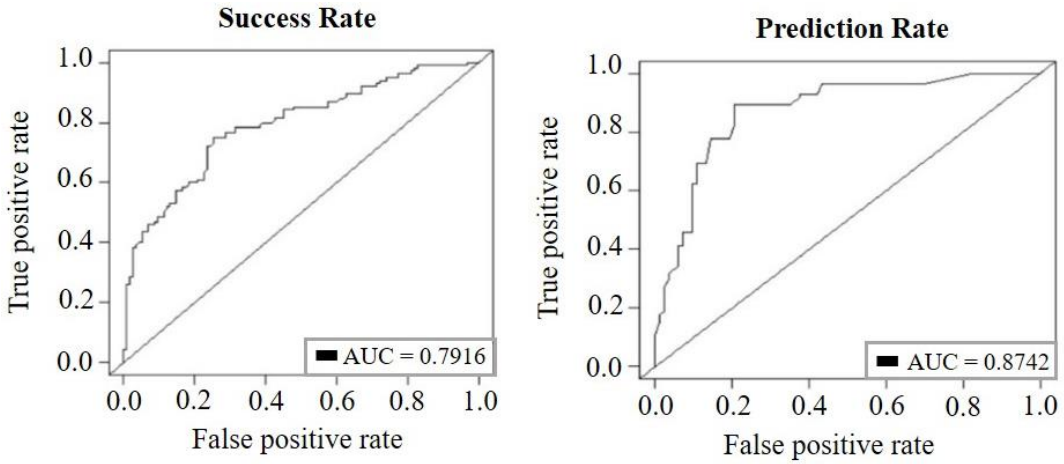

Figure 5 Success rate curve and prediction rate curve

check the success rate of the model while validation dataset is used for the prediction rate of the landslide LSM. This study uses kappa index for checking the reliability of the model and area under curve (AUC) of receiver operating characteristic (ROC) curve to evaluate accuracy of the landslide susceptibility map.

The Kappa value varies from −1 (non-reliable) to 1 (reliable). The kappa index was calculated using the Equation 5 and it indicate the reliability of the model. The kappa scales and its interpretation are ≤0(poor), 0–0.2(slight), 0.2–0.4(fair), 0.4–0.6(moderate), 0.6–0.8(substantial) and 0.8–1(almost perfect) agreement between estimation (model) and the ground reality (landslide inventory) [8]. The kappa index is calculated based on the following formula

$$Kappa = \frac{P_{obs} - P_{exp}}{1 - P_{exp}} \quad (5)$$

$$P_{obs} = \frac{TP + TN}{n} \quad (6)$$

$$P_{exp} = \frac{(TP + FN)(TP + FP) + (FP + TN)(FN + TN)}{n^2} \quad (7)$$

Where, P_{obs} is the observed agreements, P_{exp} is the expected agreements and n represent the total pixel of the training dataset, TP(true positive) and TN(true negative) are the correctly landslide and non-landslide point respectively. The FP (false positive) and FN (false negative) are the incorrectly classified landslide and non-landslides respectively [32].

The Kappa value of the model are 0.4261 and 0.5510 for the training and validation dataset respectively. Both the kappa values falls under the scale moderately agreement (0.4-0.6) between the estimation (model) and the ground observation [8]. The ROC curve is plotted using False Positive Rate on X-axis and True Positive Rate on Y-axis [32]. The success rate indicates the model fitness for the training dataset because the training data was used to build the model [18]. The prediction rate is used to evaluate the future predictive power of the LSM [33] and it was calculated using the validation dataset. The interpretation of AUC value are as follow: poor (0.5–0.6), moderate (0.6–0.7), good (0.7–0.8), very good (0.8–0.9) and excellent (0.9–1) [32]. According to the AUC (Figure 5), the success rate (0.7916) falls under good category (0.7-0.8) while the prediction rate (0.8742) falls under very good (0.8-0.9) category [32].

4. Conclusions

The landslide assessment is crucial for the future prediction of the landslide susceptible area, infrastructure development and prevention of landslides in the landslide prone areas. There are many approaches for assessing the landslide risk zone. It is important to choose simple and effective model for the generation of landslide susceptible area with higher predictive power and close to real landslide risk zone. However, the accuracy of the different approaches is still debatable. Their accuracy varies from one study area to another and based on the factor selection. For this research, the Ossey watershed area in Bhutan was chosen as the study area. The ossey watershed area experiences one of the worst landslides every year. During the monsoon season, the roads gets blocked and the local resident were cut off from the neighboring places due to landslides.

A total of 164 landslide location were identified through sentinel-2 interpretation and google earth and field visit. The

landslide inventory information was collected from the year 2017-2019 in the month of April to September. A total of 70% of the total landslides were used randomly for training dataset while remaining 30% were used for validation dataset. Total of twelve factors were selected based on availability of data. Frequency ratio model was employed for the generating LSM. The kappa index of the model was 0.4261 and 0.5510 for the training and validation dataset respectively indicating LSM was moderately reliable as per the kappa scale. The AUC result indicated the success rate was 0.7916 and the prediction rate was 0.8742 illustrating the generated LSM is good enough for the implementation for the future planning. Finally, the LSM is classified into five classes using the equally interval classifier as shown in the Figure 3. As per the equal interval classification, the high and very high-risk area were 3.82% and 0.20% of the total area, respectively.

The developed LSM in this study could help decision makers, planners, and engineers to make better decisions for the future infrastructure developmental activities avoiding the landslide risky area. The GIS-based statistical approach is cheap, simple and provide comprehensive landslide information. However, it is recommended to soil data for the future study to improve the accuracy of the LSM. It is also recommended to use other approaches and compare the accuracy of the assessment.

5. References

[1] Varnes DJ. Landslide types and processes. In: Eckel EB, editor. Landslides and engineering practice. Washington: Highway Research Board; 1958. p. 20-47.

[2] Sun X, Chen J, Bao Y, Han X, Zhan J, Peng W. Landslide susceptibility mapping using logistic regression analysis along the jinsha river and its tributaries close to Derong and Deqin County, Southwestern China. ISPRS Int J Geo-Inf. 2018;7(11):438.

[3] Shirani K, Pasandi M, Arabameri A. Landslide susceptibility assessment by dempster–shafer and index of entropy models, Sarkhoun basin, southwestern Iran. Nat Hazards. 2018;93(3):1379-418.

[4] Xiao T, Yin K, Yao T, Liu S. Spatial prediction of landslide susceptibility using GIS-based statistical and machine learning models in Wanzhou County, Three Gorges Reservoir, China. Acta Geochim. 2019;38(5):654-69.

[5] Ayalew L, Yamagishi H. The application of GIS-based logistic regression for landslide susceptibility mapping in the Kakuda-Yahiko Mountains, Central Japan. Geomorphology. 2005;65(1-2):15-31.

[6] Aleotti P, Chowdhury R. Landslide hazard assessment: summary review and new perspectives. Bull Eng Geol Env. 1999;58(1):21-44.

[7] Khan H, Shafique M, Khan MA, Bacha MA, Shah SU, Calligaris C. Landslide susceptibility assessment using Frequency Ratio, a case study of northern Pakistan. Egypt J Remote Sens Space Sci. 2019;22(1):11-24.

[8] Tien Bui D, Shahabi H, Shirzadi A, Chapi K, Alizadeh M, Chen W, et al. Landslide detection and susceptibility mapping by airsar data using support vector machine and index of entropy models in cameron highlands, Malaysia. Remote Sens. 2018;10(10):1527.

[9] Singh K, Kumar V. Hazard assessment of landslide disaster using information value method and analytical hierarchy process in highly tectonic Chamba region in bosom of Himalaya. J Mt Sci. 2018;15(4):808-24.

[10] Liu J, Duan Z. Quantitative assessment of landslide susceptibility comparing statistical index, index of entropy, and weights of evidence in the Shangnan area, China. Entropy. 2018;20(11):868.

[11] Zhao X, Chen W. Gis-based evaluation of landslide susceptibility models using certainty factors and functional trees-based ensemble techniques. Appl Sci. 2020;10(1):16.

[12] Hussain G, Singh Y, Singh K, Bhat G. Landslide susceptibility mapping along national highway-1 in Jammu and Kashmir State (India). Innov Infrastruct Solut. 2019;4(1):59.

[13] Pasang S, Kubíček P. Information value model based landslide susceptibility mapping at Phuentsholing, Bhutan; AGILE conference 2018; 2018 Jun 12-15; Lund, Sweden. p. 1-6.

[14] Sarkar R, Dorji K. Determination of the probabilities of landslide events—a case study of Bhutan. Hydrology. 2019;6(2):52.

[15] Sarkar R, Kurar R, Zangmo S, Dema U, Subba S, Sharma D. Application of soil nailing for landslide mitigation in Bhutan: a case study at Sorchen Bypass. Electron J Geotech Eng. 2017;22(13):4963-80.

[16] Cheki D, Shibayama T. Method for landslide risk evaluation and road operation management: a case study of Bhutan. J Construct Manag. 2008;15:23-31.

[17] Pourghasemi HR, Pradhan B, Gokceoglu C. Application of fuzzy logic and analytical hierarchy process (AHP) to landslide susceptibility mapping at Haraz watershed, Iran. Nat Hazards. 2012;63(2):965-96.

[18] Nohani E, Moharrami M, Sharafi S, Khosravi K, Pradhan B, Pham BT, et al. Landslide susceptibility mapping using different GIS-based bivariate models. Water. 2019;11(7): 1402.

[19] Long S, McQuarrie N, Tobgay T, Grujic D, Hollister, L. Geologic map of Bhutan. J Map. 2011;7(1):184-92.

[20] Pourghasemi HR, Moradi HR, Fatemi Aghda SM, Gokceoglu C, Pradhan B. GIS-based landslide susceptibility mapping with probabilistic likelihood ratio and spatial multi-criteria evaluation models (North of Tehran, Iran). Arab J Geosci. 2014;7:1857-78

[21] Lee S, Min K. Statistical analysis of landslide susceptibility at Yongin, Korea. Environ Geol. 2001;40(9): 1095-113.

[22] Youssef AM, Pradhan B, Pourghasemi HR, Abdullahi S. Landslide susceptibility assessment at Wadi Jawrah Basin, Jizan region, Saudi Arabia using two bivariate models in GIS. Geosci J. 2015;19(3):449-69.

[23] Moore ID, Grayson R, Ladson A. Digital terrain modelling: a review of hydrological, geomorphological, and biological applications. Hydrolog Process. 1991;5(1):3-30.

[24] Chen FW, Liu CW. Estimation of the spatial rainfall distribution using inverse distance weighting (IDW) in the middle of Taiwan. Paddy Water Environ. 2012;10(3):209-22.

[25] Childs C. Interpolating surfaces in ArcGIS spatial analyst. ArcUser. 2004:32-35.

[26] Lee S, Talib JA. Probabilistic landslide susceptibility and factor effect analysis. Environ Geol. 2005;47(7):982-90.

[27] Jaafari A, Najafi A, Pourghasemi H, Rezaeian J, Sattarian A. GIS-based frequency ratio and index of entropy models for landslide susceptibility assessment in the Caspian forest, northern Iran. Int J Environ Sci Technol. 2014;11(4):909-26.

[28] Park S, Choi C, Kim B, Kim J. Landslide susceptibility mapping using frequency ratio, analytic hierarchy process, logistic regression, and artificial neural network methods at the Inje area, Korea. Environ Earth Sci. 2013;68(5):1443-64.

[29] Meten M, PrakashBhandary N, Yatabe R. Effect of landslide factor combinations on the prediction accuracy of landslide susceptibility maps in the Blue Nile Gorge of Central Ethiopia. Geoenviron Disasters. 2015;2(1):9.

[30] Osaragi T. Classification methods for spatial data representation. CASA. 2002:1-19.

[31] Kaur H, Gupta S, Parkash S, Thapa R, Gupta A, Khanal GC. Evaluation of landslide susceptibility in a hill city of Sikkim Himalaya with the perspective of hybrid modelling techniques. Ann GIS. 2019;25(2):113-32.

[32] Shirzadi A, Bui DT, Pham BT, Solaimani K, Chapi K, Kavian A, et al. Shallow landslide susceptibility assessment using a novel hybrid intelligence approach. Environ Earth Sci. 2017;76(2):60.

[33] Wang Q, Li W, Chen W, Bai H. GIS-based assessment of landslide susceptibility using certainty factor and index of entropy models for the Qianyang County of Baoji city, China. J Earth Syst Sci. 2015;124(7):1399-415.